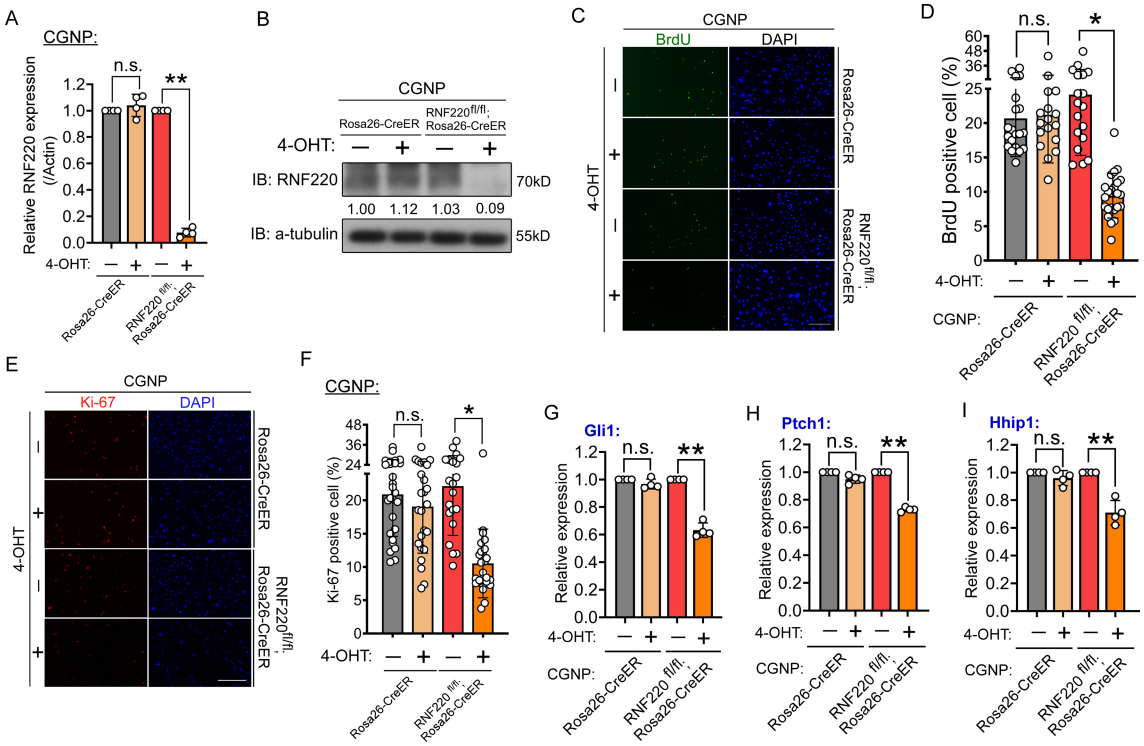

Figure S1. RNF220 knockout inhibits CGNP proliferation. (A and B) Real-time PCR (A) and western blotting (B) showing the 4-OHT induced RNF220 knockout effiency in CGNP cells. IB, immunoblot. (C-F) BrdU incorporation (C and D) and Ki-67 (E and F) staining assays to evaluate DNA synthesis and proliferation rates of CGNPs when RNF220 was knocked out by 4-OHT induction. Scale bar, 80 μm. Quantification were shown in (D) and (E) respectively. (G-I) Realtime PCR assays show the relative expression level of Gli1(G), Ptch1 (H) and Hhip1 (I) in CGNP cells when RNF220 knokout was induced by 4-OHT incubation or not. Data are presented as the means ± SD. n.s., no significant difference; * $p < 0.05$; ** $p < 0.01$.

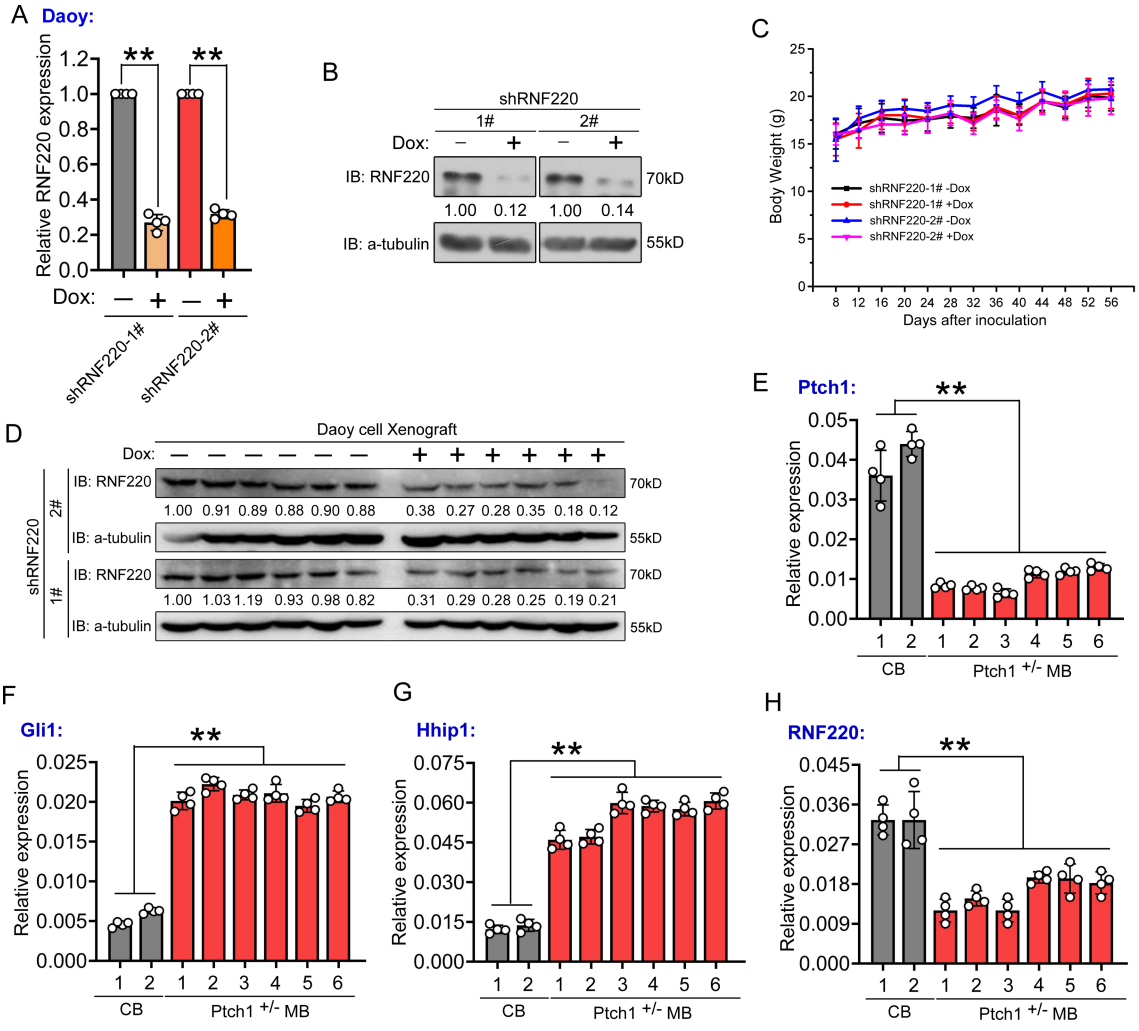

Figure S2. RNF220 knockdown efficiency and mRNA levels of Gli1, Ptch1, Hhip1 and RNF220 in Ptch1$^{+/-}$ MB tissues. (A and B) Real-time PCR (A) and western blotting (B) showing the Dox-induced RNF220 knockdown efficiency in shRNF220-1# or 2# stable Daoy cell lines. (C) Mice body weight was measured every four days after shRNF220-1# or 2# clones were injected subcutaneously into BALB/c nude mice and mice were feeded with or without Dox. (D) RNF220 protein levels in tumor tissues were detected by western blotting. The protein level was quantified against α-tubulin followed by each control and the statistics were shown below each panel. IB, immunoblot. (E–H) Real-time PCR of the relative expression of Ptch1 (E), Gli1 (F), Hhip1 (G) and RNF220 (H) in control cerebellum and Ptch1$^{+/-}$ MB tissues. Data are presented as the means ± SD. ** $p< 0.01$.

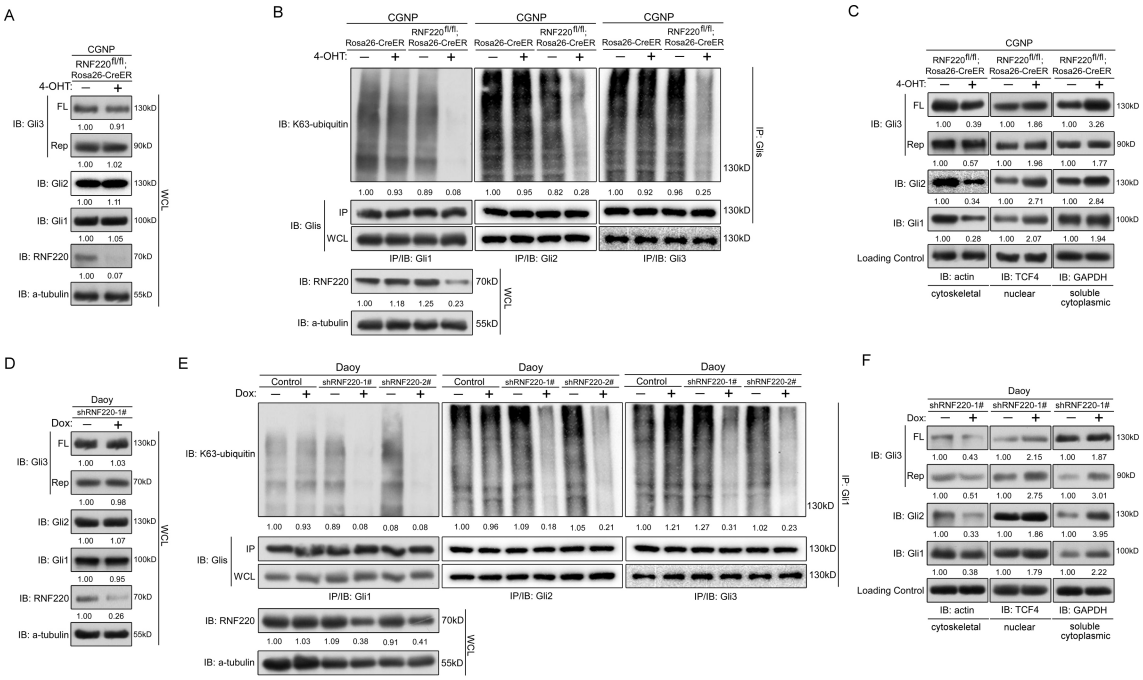

Figure S3. RNF220 targets Glis for K-63 linked polyubiquitination and promotes its nuclear exportation in both CGNPs and Daoy cells. (A) Western blot results showing the effect of RNF220 knockout on all the Glis protein level in CGNP cells. (B) The level of K-63 ubiquitinated Glis in the CGNP cells when RNF220 was induced knockout or not. (C) Western blot assays showing the subcellular distribution of endogenous Glis in control or RNF220 knockout CGNP cells. (D) Western blot results showing the effect of RNF220 knockdown on all the Glis protein level in Daoy cells. (E) The level of K-63 ubiquitinated Glis in the Daoy cells when RNF220 was induced knockdown or not. (F) Western blot assays showing the subcellular distribution of endogenous Glis in control or RNF220 knockdown Daoy cells. The protein level was quantified against α-tubulin followed by each control and the statistics were shown below each panel. IP, immunoprecipitation; WCL, whole cell lysate; IB, immunoblot.

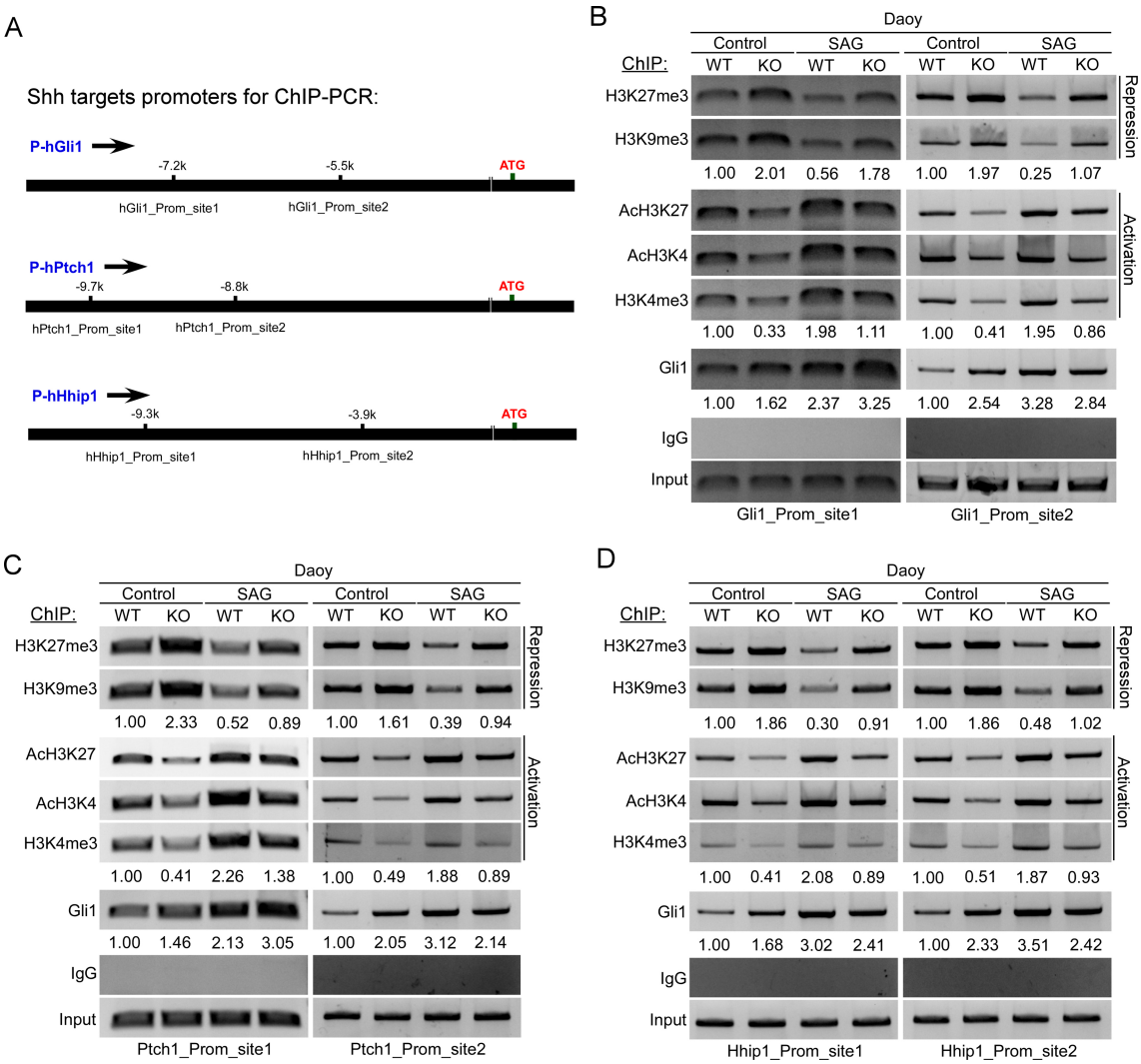

Figure S4. RNF220 knockdown alters epigenetic modification on the promoter of Shh signaling targets in Daoy cells. (A) Schematic representation of the tested Gli binding sites in mouse Gli1, Ptch1 and Hhip1 promoters. The coordinates refer to the translational start codon. (B-D) Semi-quantifiction ChIP-PCR analysis of histone modification marks at the indicated Gli binding sites in Gli1 (B), Ptch1 (C) and Hhip1 (D) promoters in Daoy cells when endogenous RNF220 was knocked down. Dox was used to induce endogenous RNF220 knockdown in shRNF220 stably transfected Daoy cells. Note that for each repressive or activating group, the averaged relative levels of the different marks were shown.

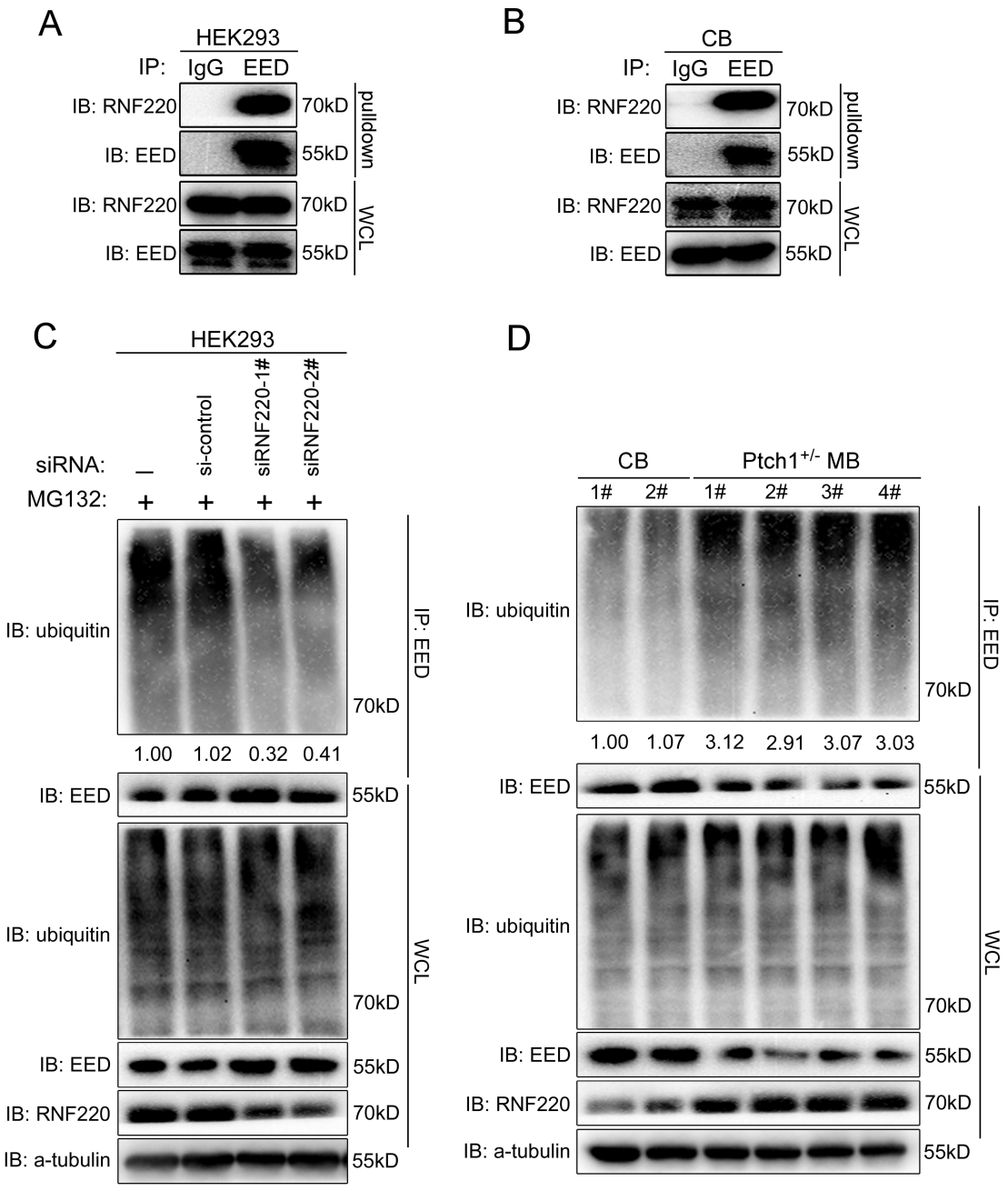

Figure S5. RNF220 interacts with EED and targets EED for polyubiquitinaion and degradation. (A and B) Endogenous RNF220 was pulled down by EED in both HEK293 cells (A) and control cerebellum (B). (C) The polyubiquitination level of endogenous EED protein reduced when RNF220 was knocked down in HEK293 cells. (D) The ubiquitination level of endogenous EED protein in control cerebellum and Ptch1$^{+/-}$ medulloblastoma tissues. The protein level was quantified against α-tubulin followed by each control and the statistics were shown below the indicted panels. WCL, whole cell lysate. IP, immunoprecipitation. IB, immunoblot.

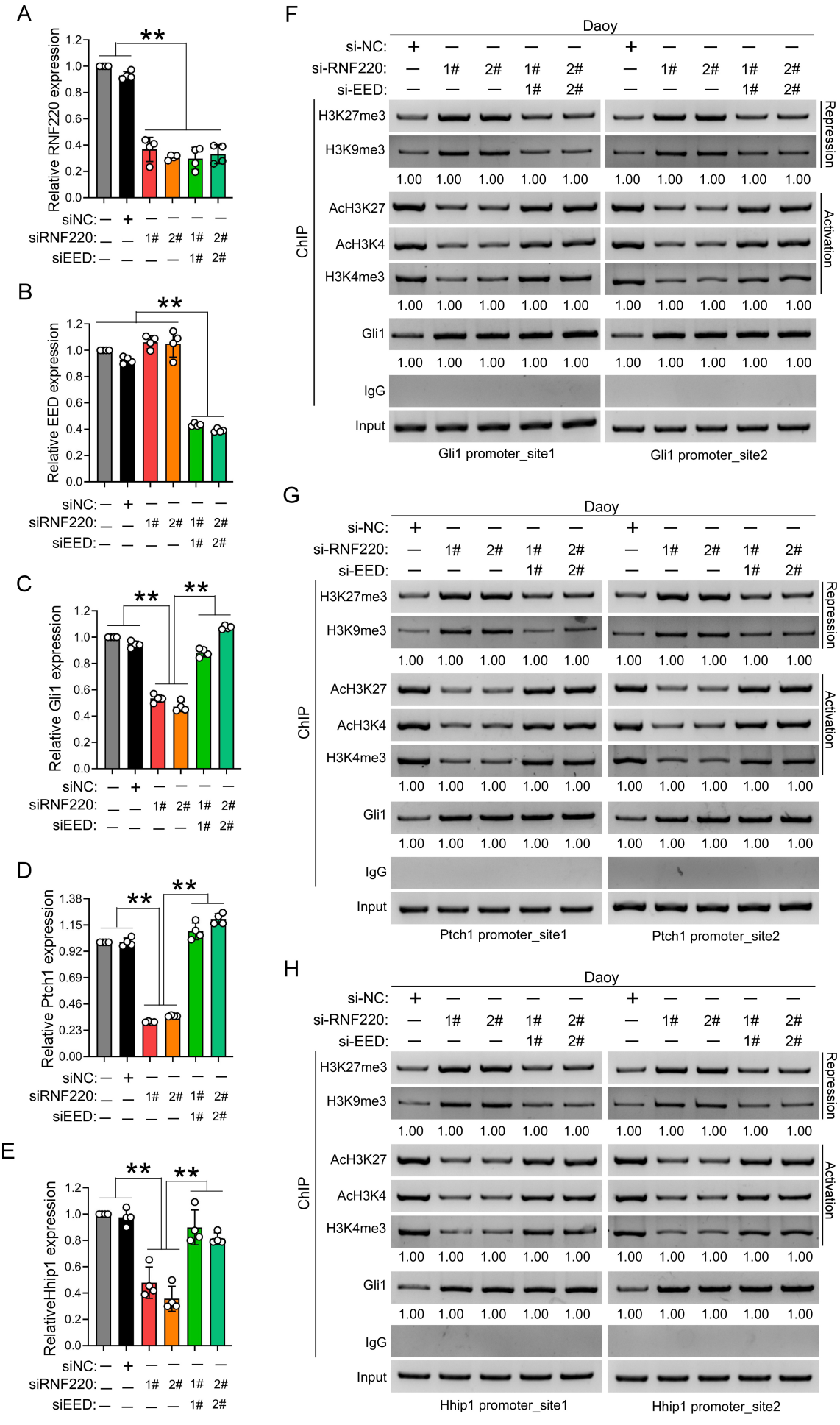

Figure S6. EED knockdown rescue RNF220 knockdown mediated Shh signaling repression and epigentic modification changes on the promoters of Shh signaling targets in Daoy cells. (A-E) Realtime PCR assays showed the relative expression level of RNF220 (A), EED (B), Gli1 (C), Ptch1 (D) and Hhip1 (E) when the indicated siRNAs were transfected into the Daoy cells. (F-H) Semi-quantification ChIP-PCR analysis of histone modification marks at the indicated Gli binding sites in Gli1 (F), Ptch1 (G) and Hhip1 (H) promoters in Daoy cells. The indicated siRNAs were used to knockdown the endogenous RNF220 or EED in Daoy cells. Cells were harvested at 72 hours after siRNAs transfection and followed by nuclear purification, chromosome fragments and immuniprecipitation with the indicated antibodies. Note that for each repressive or activating group, the averaged relative levels of the different marks were shown.

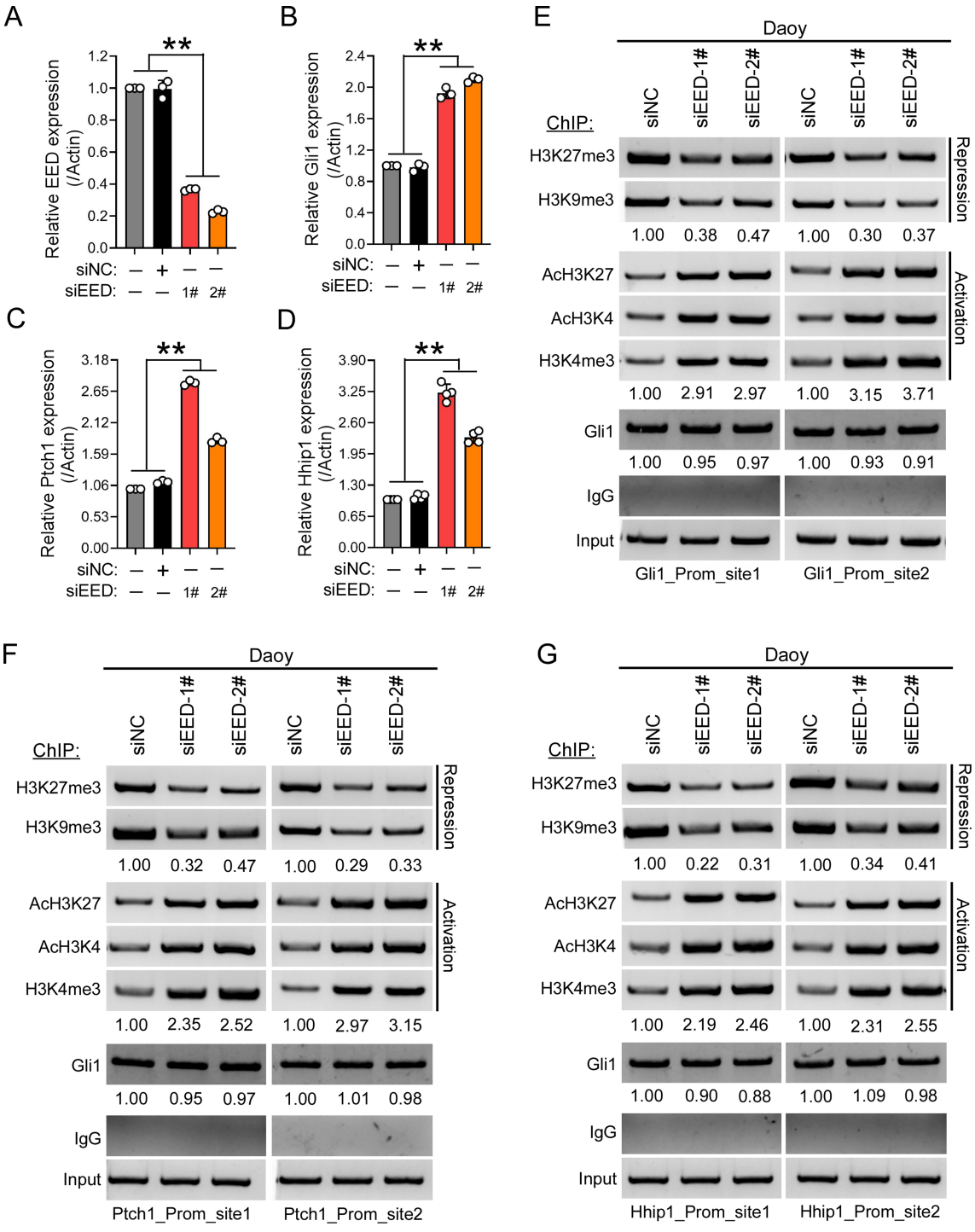

Figure S7. EED knockdown inhibits Shh signaling and changes the epigenetic modification on the promoters of Shh signaling targets in Daoy cells. (A-D) Realtime PCR assays showed the relative expression level of EED (A), Gli1 (B), Ptch1 (C) and Hhip1 (D) when the endogenous EED was knocked down in Daoy cells. (E-G) Semi-quantification ChIP-PCR analysis of histone modification marks at the indicated Gli binding sites in Gli1 (E), Ptch1 (F) and Hhip1 (G) promoters in Daoy cells when endogenous EED was knocked down. Note that for each repressive or activating group, the averaged relative levels of the different marks were shown.

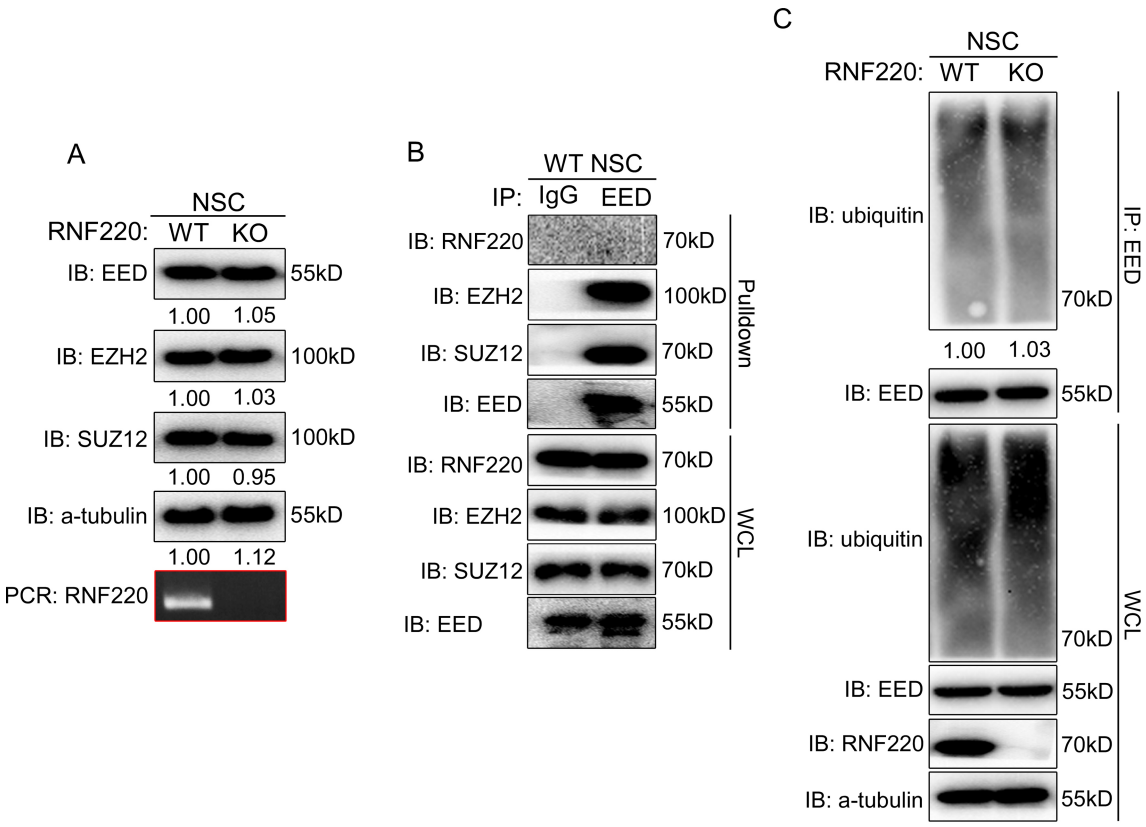

Figure S8. Effect of RNF220 knockout on EED protein levels and epigenetic modification of Shh target genes in NSCs. (A) Western blotting of the PRC2 complex protein levels in control and RNF220 knockout NSC. (B) Co-IP assays shows the interaction between EED and the indicated proteins. In NSC, EED could pull down the other PRC2 complex member, such as EZH2 and SUZ12, but not RNF220. (C) The polyubiquitination level of endogenous EED is comparable between wildtype and RNF220 knockout NSC. The protein level was quantified against α-tubulin followed by each control and the statistics were shown below the indicated panel. IB, immunoblot; IP, immunoprecipitation; WCL, whole cell lysate.

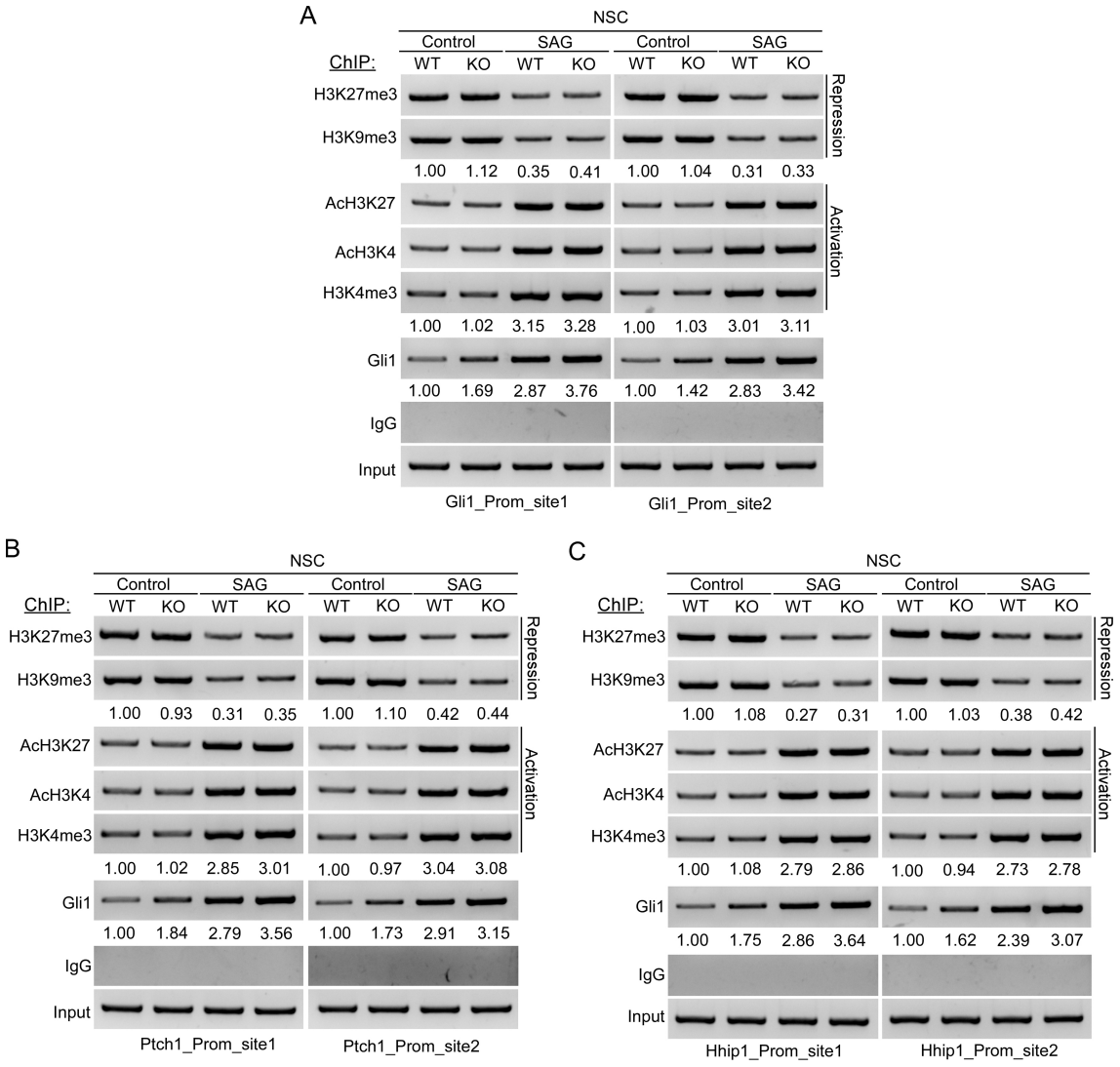

Figure S9. Effect of RNF220 knockout on epigenetic modification marks at Gli binding sites in NSCs. Semi-quantification ChIP-PCR analysis of histone modification marks at the indicated Gli binding sites in the mouse Gli1 (A), Ptch1 (B) and Hhip1 (C) promoters in control or RNF220 knockout NSC. Note that for each repressive or activating group, the averaged relative levels of the different marks were shown.